Concrete Beton

Number 123
November 2009

The Official Journal of
The Concrete Society
of Southern Africa

Platinum member: NPC - Cimpor

Accredited technical paper:
Constitutive model for fibre-reinforced strain hardening cement composites (SHCC)

Concrete Chatter
Inland Concrete Boat Race
KZN's Egg Protection Competition
Western Cape Cube Competition

NPC
CIMPOR

President's Message

The other day, while going through a diving manual for a course that I am instructing, I found a significantly profound quote by Confucius: "Tell me and I will forget, show me and I will remember, **involve** me and I will understand."

I couldn't help pondering upon this for quite some time. The longer I did, the more I realised what a gem it is and how pertinent it is in the South African-built environment context.

We are currently struggling with the colossal task of transferring skills to our enormous potential labour force.

Gone are the days of apprenticeships when one was trained and mentored for anything up to five years before being deemed worthy of receiving the relevant artisan qualification.

A three week course, I am afraid, cannot provide one with the in-depth understanding of the trade which one has chosen. At the very best, it provides the bare minimum to start out in a certain field of work, and no more. The rest must be learned on the job.

I recall reading the statistics on the number of qualified tradesmen in our country about two years ago and was absolutely astonished and horrified to learn the actual percentage of people now available and actively still working in South Africa, relative to say tradesmen in the early to mid- eighties. With so few senior tradesmen (or should I say trades-people) available, skills transference and mentorship to the youth presents a serious uphill battle for the foreseeable future.

In my experience, young engineers and technicians, having just emerged from the hallowed halls of their respective Alma Mater, if they can actually find employment, quite often find themselves thrown into a wild construction industry, without much in the way of structured mentoring regimes being available to them. It's a real "sink or swim" situation for many of our fledgling technical people.

This brings me to the point of professional engineering personnel. Currently I understand the average age of Registered Professional Engineers and Engineering Technologists to be around 57 years - this age group represents the overwhelming majority. What I also understand from one of my esteemed colleagues working and lecturing at one of the major tertiary institutions, is that due to the recent economic and building boom, the class sizes have experienced unprecedented growth over the past few years.

Now here is the conundrum – What do we do as a country in eight or so year's time when the majority of these folk retire? The current economic downturn will in all probability serve to amplify the problem. It may be that skills transfer and mentoring take a back seat to survival in many companies for the time being, unfortunately. We need to collectively ensure that all students who qualify, be it with a degree or diploma, be given a fair shot at developing a career in our industry.

Even more importantly, we must utilise and draw from the sagely skills of our "older" engineering and other technical mentors to the maximum benefit to our youth and our Country.

The Society can play in assisting your company with some of the skills transfer portions of this mentoring process, with the high quality and varied in nature, technical talks, seminars, symposia and conferences that we host.

This is your Society- use its facilities!

I would like to take this opportunity to wish all our members and other readers of this Journal a relaxing and joyous festive season, a safe passage if you are travelling and a vibrant New Year.

Francois Bain Pr Eng
President:
The Concrete Society of Southern Africa

Cover: The iconic Soccer City is the largest stadium in Africa and seats 89 000. The stadium was built by Aveng Group subsidiary, Grinaker-LTA /Interbeton by Soccer City Joint Venture.

The iconic Soccer City

The iconic Soccer City, African calabash pot design, won the prestigious Fulton Awards for 'Concrete in Architecture' and captured a second Fulton Award for winning the 'Building Project' award.

The roof wetting for Johannesburg's latest landmark was auspiciously marked by a downpour and in traditional African style, dignitaries, contractors and workers celebrated the start of the final completion inspections of Soccer City.

The 89 000-seater, African stadium will host both the opening and final matches of the 2010 FIFA World Cup matches. The stadium is the largest in Africa. It is also the biggest all-seated stadium built for any football world cup event.

The Team from Grinkaker–LTA/Interbeton by Soccer City Joint Venture; the client the City of Johannesburg – 2010 Office; principal agent Phumela Africa Professional Engineers and subcontractors DSE, Steeldale Reinforcing and Fixing Services, Ground Engineering joined the work force in celebrations.

Roger Jardine, CEO of the Aveng Group and its subsidiary Grinaker-LTA, said at the roof wetting, "we are immensely proud of this landmark development. Not only does it highlight African design and ingenuity but this was achieved with 1million disabling injury-free man hours – an unprecedented achievement under such tight deadlines." He proudly added that this bares testament to Aveng and its partners' unrelenting focus on safety.

Building the stadium required 90 000 m^3 of concrete steel, about 10 000 tons of reinforced steel, 9 million bricks and 13 000 tons of structural steel. The structure has a double layer of fabric roof and required 32 400 fibre cement panels to complete the calabash-inspired design of the façade.

Fulton Awards winner

It has taken some 9 980 000 hours to complete the construction of Soccer City, since the project's inception in 2007, says Mike Moody, Grinaker–LTA project director.

Grinaker-LTA MD, Neil Cloete says that the initial bid was to complete Soccer City with a simple roof.

The organising committee wanted a meaningful African design, and it is incredible to have witnessed the transformation of the site into what will be a landmark for the country and the continent at large.

Every seat in the stadium has an unrestricted view of the pitch and the grounds, with the furthest seat 105m from the centre of the pitch.

There are 193 suites and roughly 2 700 seats dedicated solely to media, 860 parking bays and 77 concession kiosks. Particularly black-marked seats form lines pointing in the direction of other stadiums around the country where World Cup matches will be played.

Motivation: Architectural design description

The architectural design of the stadium was selected from a series of concept designs, ranging from acknowledgement of Jo'burg's disappearing mine dumps; the kgotla (defined by the tree) of the African city state; the African map as a horizontal representation, which included the roof as a desert plain supported on tropical trees set within the mineral wealth of Southern African; to a representation of the protea, our national flower.

The calabash, or African pot design, proposed by Boogertman Urban Edge and Partners, was selected as being the most recognisable object to represent what would automatically be associated with the African continent and not any other. The calabash, or 'melting pot of African cultures', sits on a raised podium, on top of which is located a 'pit of fire'. Thus the pot sits in a depression, which is the 'pit of fire', as if it were being naturally fired. The pit of fire demarcates the security and turnstile line separating the outer areas and the secure inner areas.

The structural profile of the existing suite levels and upper-tier seating of the existing western grandstand are extended all round to encircle the pitch. The existing lower embankment will be rebuilt to vastly improve the view lines and comfort of the most popular seats in the house. The upper third of the existing embankment is to be raised to form a secondary tier, thus turning the stadium into a 3-tiered, rather than a 2-tiered, stadium. The upper embankment and the rebuilt lower embankment are accessible from the lower concourse, which is fed from the podium level.

The two suite levels and the upper tier are accessed via 3-dimensional ramp structures that are contained within the façade of the pot. The suite levels also have separate lift and stair lobbies at each corner for dedicated secure VIP access.

The Calabash African pot design

The pot's façade is made up of laminated fibre reinforced concrete panels, in a selection of 8 colours and 2 textures that make reference to the shades and textures of the calabash. The pot is punctured by open or glazed panels which create a suggestion of pattern on the façade that comes into its own when the inside volumes are illuminated. The façade is articulated by 10 vertical slots which are aligned geographically with the nine other 2010 stadia, as well as the Berlin stadium. These are representative of the road to the final, and it is hoped that, after the World Cup, the scores of each game at each venue will be placed in pre-cast concrete panels on the podium. A visit to the stadium will thus provide one with a full history of the World Cup and all its scores.

The upper roof, which is cantilevered from an enormous triangular spatial ring truss, is covered by a PTFE membrane in a colour similar to that of the adjacent mine-dump sand. The bottom of the trusses will be covered by a perforated mesh membrane, thus giving the appearance of a smooth under-slung ceiling. All VIP areas and the stadium management offices will be located behind the main western grandstand, with a dedicated VIP entrance. New change rooms, media work areas, auditorium, and VIP parking are located within a new basement under the podium on the western side of the stadium.

The site is directly north of the proposed new Nasrec Transportation Hub and pedestrian mall, linking the stadium to the redeveloped Expo Centre to the south.

The transportation hub will accommodate taxi, bus, and rapid transit services, thus providing good public transport links to the precinct and the stadium.

A secondary Bus Rapid Transit station is also proposed on the Soweto highway to the north of the stadium, which will further strengthen the public transport links to the stadium.

All of this is to be set in a revamped Nasrec precinct, which will boast new roads, and pedestrian walkways with lighting, signage, landscaping, CCTV, and public amenities.

Mike Moody, Grinaker-LTA project director

Structural Design

P.D. Naidoo & Associates (PDNA) are the principal structural engineers for the upgrading of Soccer City. PDNA appointed a German company, Schlaich Bergermann & Partners, as a specialist roof sub-consultant to assist with the detail analysis and design of the roof and façade structures. The existing stadium, which was first constructed in 1987, consisted of a playing field surrounded by embankment seating, two levels of corporate hospitality suites, and an elevated seating tier on the western side only.

Aveng CEO Roger Jardine

The architects for this prestigious project, Boogertman Urban Edge and Partners, in association with HOK Sports Architecture, have created, an "African Pot" which will in future be recognized instantly by spectators in every corner of the world. To achieve this unique look, a structure, circular in shape on plan, was created to envelope the upgraded triple-tiered concrete seating bowl.

The circular plan format of the pot, which encircles the rectangular seating bowl and field, was selected to ensure that all façade detailing could be consistent in plan and section, thus ensuring an easier detailing, manufacture, and installation process. This ensured that the 120 concrete façade columns would be consistent in shape and form. Given that the existing concrete structure was limited in its ability to carry the additional roof load imposed on it, it was

Winning building project

decided by the design team to remove the roof structure from the seating bowl structure and place the roof structure on 12 off-shutter concrete shafts. These shafts required an ingenious piling solution.

Piling

On completion, approximately 1350 piles will have been installed at Soccer City. The forces generated by the concrete structure and roof mean that exceptionally high loads have been transferred to the foundations, which has resulted in the design and construction of some of the most extreme piles ever installed in South Africa. All the piles and lateral support were designed by ARQ and Verdicon, and installed by GEL.

Whilst many of the piles carry large compressive loads, many piles are also subjected to exceptionally high tension loads. The calabash-shaped façade and the roof transfer the loads from the roof, down twelve reinforced concrete shafts and 120 inclined perimeter façade columns, to the piled foundations. Some shaft foundations are required to resist tension loads up to 13000kN, in combination with sheer loads of 6000kN and a bending moment of 125000kNm. Due to the limited space, it was only possible to install a maximum of 12 piles per shaft foundation, resulting in some piles being subjected to tension loads of 5800kN (580 tons). In order to accommodate the massive loads, the designers decided to anchor the piles 6m into the sandstone bedrock using dowel bars installed through the base of the pile.

In some cases the 1500 diameter piles were installed up to a depth of 33m, necessitating almost 60m^3 of concrete in a single pile.

Shafts

The roof is supported by 12 large, 40m-high rectangular concrete shafts, each of which is designed to withstand large horizontal and vertical loads. The shafts vary in plan from 3.5m x 5.0m to 3.5m x 14.0m, with an average wall thickness of 600mm. A huge reinforcing steel content of 460kg/m^3 (approximately

Grinaker-LTA Managing Director, Neil Cloete

Largest stadium in Africa

three times more than normal reinforced concrete) made the placing and compaction of the concrete extremely difficult. The stiffness of the shafts under varying load combinations had to be determined accurately, as this could affect the forces in the structural steel roof structure. The design and stiffness of the shafts were further complicated by various openings which had to be provided for electrical, mechanical, fire, domestic, and storm water services. All these services were designed early on in the process and modelled in 3D by the architects to ensure that all penetrations were fully co-ordinated, before the reinforcing was designed by the engineers. This was required as it was impossible to entertain any late requests for penetrations by the services engineers. These shafts are founded on the piled foundations described above, with some piles subjected to downward loads of 1100 tons and upward loads of 580 tons. In addition to the shafts, 16 circular columns of 1 meter diameter support the roof.

Shaft bases

In order to transfer the large loads from the roof, via the concrete shafts, into the tension and compression piles, large pile caps with depths in excess of 4m were required. The construction of these large bases required careful planning, as heat of hydration had to be controlled, and the safety of construction workers, who are often required to work beneath heavy reinforcement, had to be ensured. Varying soil conditions on site often required that the engineers had to adapt the design of these bases.

Lateral Support

To allow access into the completed stadium bowl, three deep tunnels had to be cut with vertical excavation. The western players' tunnel runs below the existing stadium structure, and has permanent support with a maximum vertical height of up to 10.0m. The south-west and north-east tunnels have been constructed through new portions of the stadium. Due to programming constraints, it was decided to construct permanent lateral support in these tunnels, consisting of soil nails, shotcrete, and mesh. Due to the construction of deep pile caps at the base of the north eastern tunnel, vertical lateral support heights of up to 13.0m have been constructed.

Raking Beams

In order to vastly improve the sightlines of the existing stadium, the rake of the existing western upper tier has been increased, and an additional raised seating tier has been introduced on the upper portion of the embankment. Two levels of hospitality suites and the upper tier have been completed on the northern, eastern, and southern pavilions, thereby creating a classic triple–tiered bowl. All raking beams were constructed using purpose-made formwork. The existing pre-cast steppings to the western upper tier were removed, crushed, and recycled as base layers for the bulk earthworks. All new seating steppings are constructed from pre-cast concrete, all made on site.

Pre-Cast yard and pre-cast elements

To reduce the handling time and damage to precast units, as well as to achieve a value-for-money product, GLTA/Interbeton elected to establish an on-site batching plant and pre-cast yard. This allowed for easy inspection and control of the units, which were all unique in dimension due the existing geometry of the old stadium bowl, allowing them to be placed correctly with the minimum amount of handling.

Façade Columns

One of the most challenging elements of the concrete structure was the design and construction of the façade columns. The façade structure is supported on 120 inclined concrete columns enveloping the stadium. The columns are 16.3m high, and the top of each of these columns has a horizontal eccentricity of 6.5 metres in relation to its base, resulting in large moments

and upward loads on the piled foundations. Due to the large moments and forces in these slender columns, the reinforcing steel is extremely dense (860 kg/m³), which made the use of a vibration poker extremely difficult. GLTA/Interbeton opted to use self-compacting concrete to construct these columns. All façade columns are connected with tie beams which act in ring tension so as to limit long-term deflection of the columns and façade structure. The design and construction of the façade columns had to be planned and executed very carefully, with temporary propping and bracing, so as to prevent deflection during construction. It is interesting to note that the temporary steel required for the live and dead ends of the façade columns will be recycled by the architects, with the help of a group of artists, into artworks that will have pride of place on the podium and within the Nasrec precinct.

Façade cladding

The final selection of the façade material came about after an extensive search by the architects to select a product that would ultimately reflect the nature of the concept of the calabash. Having discarded ideas of composite aluminium, steel, and various roof-sheeting options, the architects were coincidently introduced to an extruded fibre reinforced concrete panel called Fibre C, from Rieder Elements in Austria. The product is supplied in panels with varying surface finishes, honed and sandblasted, in combination with a variety of earthy colours, to create the unique variegated façade cladding. The panels, which are light-weight and only 13mm in thickness, are supplied in 1200 x 1800mm typical panel sizes and are fixed to a galvanised steel sub frame. The panels, furthermore, have excellent thermal properties and have been subjected to rigorous testing, including hail impact, water penetration, and discolouration tests.

Ramps

Eight large pedestrian ramps, designed for the efficient ingress and egress of spectators to the upper levels of the stadium, have been provided. These ramps, which also provide vehicular access to all levels, follow the shape of the façade bowl and consequently change position in plan from one level to the next. In addition to the sloped façade columns, the other columns supporting the ramps are inclined, thereby requiring intricate design analysis and construction techniques.

Training

Due to the critical skills shortage in the construction industry, the Soccer City project embarked on an extensive training initiative to provide the necessary skills required by the project and to contribute to the development of the local community. A self-sustaining training centre was established by the Soccer City project near the site, in conjunction with a black economic empowerment (BEE) training provider. Training was conducted in the following disciplines, according to the relevant unit standards: Crane Operations, Shutterhand, Concrete hand, Construction Supervisor, Foreman, Construction Plant Operator.

All new trainees were assessed through a Learner Ability Battery Test, which is non-discriminatory and is used to determine literacy, numeracy, and the development potential. All currently employed core and limited-duration employees are offered the opportunity for further training and development to enhance their skills and further their construction careers. The training centre assessed 907 unemployed learners and trained 798 learners. A large number of the unemployed learners were offered employment at Soccer City.

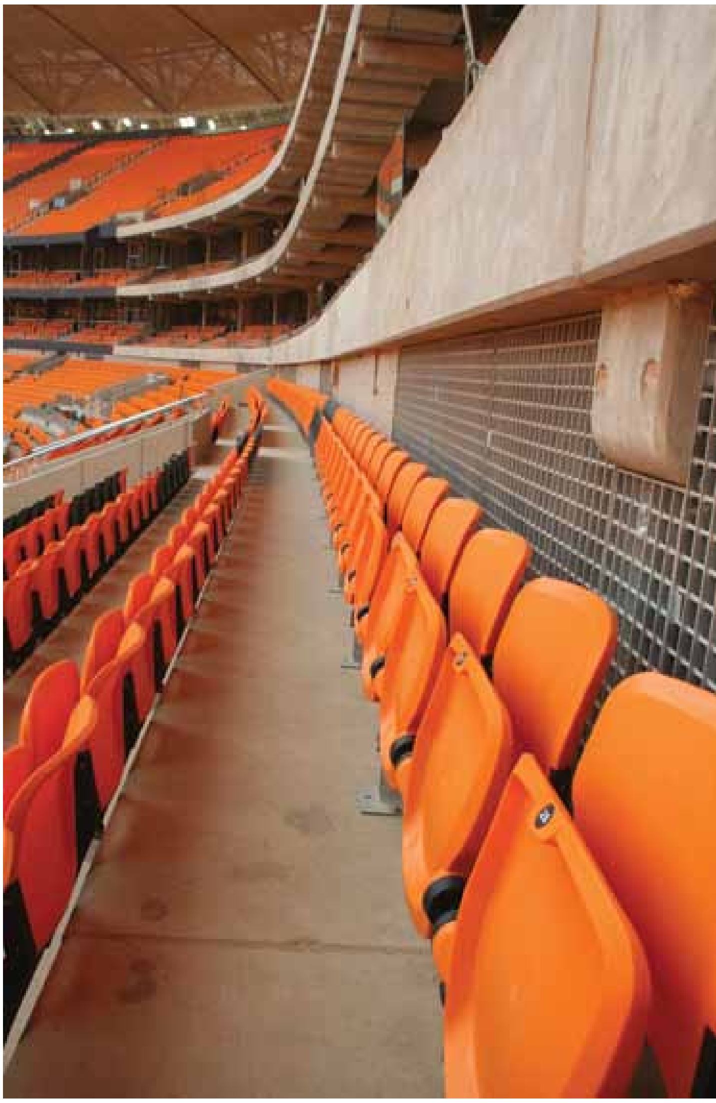

Social Upliftment

As part of their Corporate Social Investment programmes, GLTA/Interbeton have agreed to construct two classrooms at the Bella Primary School in Soweto, opposite the Hector Pieterson Museum.

ACCREDITED TECHNICAL PAPER

Constitutive model for fibre-reinforced strain-hardening cement composites (SHCC)

By GPAG van Zijl
Department of Civil Engineering, Stellenbosch University, South Africa

ABSTRACT: Constitutive models that capture dominating mechanisms of mechanical and time-dependent behaviour of construction materials are essential for accurate structural analysis. Such models may be highly complex, as the behaviour of especially cement-based construction materials is indeed complex.
The value of such models lies in the ability it affords the specialist to predict structural behaviour beyond that measured in physical experiments, which is a cost-effective extension of the physical experimental data.
With the aid of such complex models, thorough understanding and eventual simpler analytical models can be derived.
This paper describes a constitutive model for fibre-reinforced strain-hardening cement composites (SHCC).


GPAG van Zijl

SHCC is a relatively new class of high performance fibre-reinforced cement-based composites (HPFRCC), which currently receives intensive research attention internationally. Physical evidence of rate and time-dependence of SHCC is presented in terms of tensile rate-dependent test results, as well as tensile creep test results. A model for time-dependent mechanical behaviour of SHCC is proposed and elaborated. The model is based in multi-surface, anisotropic, computational continuum plasticity. It is shown to realistically capture rate-enhanced tensile resistance, as well as tensile creep fracture.

1 INTRODUCTION

This paper proposes a constitutive model for fibre re-inforced strain-hardening cement composites (SHCC). This class of high performance fibre reinforced cement composite (HPFRCC) is designed for large tensile strain capacity at moderate tensile strength, with examples shown in *Figure 1*. A high tensile strength FRCC is also shown in the figure.

The tensile ductility of SHCC is obtained through balanced fibre and matrix properties, to allow effective crack bridging by fibres, whereby cracks are controlled to widths in the micro-range, despite moderate fibre volume levels ($1.5<V_f<2.5\%$). Evidence is emerging that the crack control is maintained also in more general loading conditions, including flexure, shear (Shang & van Zijl 2007) and combined flexure and shear, both in pure SHCC and with steel bar reinforcement (R/SHCC) (van Zijl 2008).

The significance of the crack control is reduced water and chloride diffusivity through crack width limitation in cement composites, as reported by several researchers (Wang *et al*. 1997, Rapoport

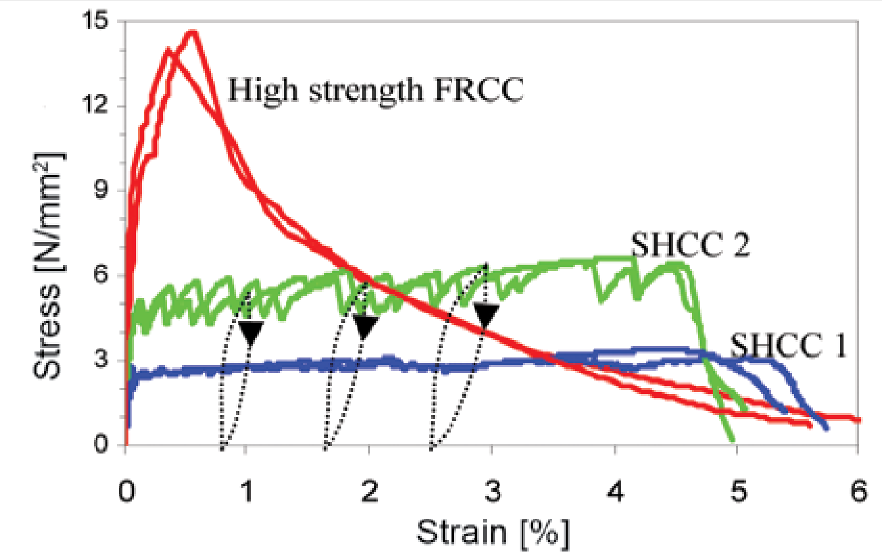

Figure 1: Tensile stress-strain responses of SHCC.

Ingredient	Mass proportion	kg/m³
Cement (CEM I 42.5)	0.5	531
Fly Ash	0.5	531
Water	0.4	425
Sand (φ_s<0.21 mm)	0.5	531
PVA fibre, L_f = 12 mm, d_f = 0.04 mm	0.024	26

Table 1: Typical SHCC mix proportions

et al. 2001, Lepech & Li 2005, Sahmaran *et al*. 2007).

These processes govern the longer term migration of water and chlorides into the material through the micropores (Bažant, & Najjar 1971, Neithalath 2006).

Under service conditions, which inevitably include cracks in cement composites, long term durability is controlled by reduced diffusivity. The experimental evidence that crack widths may be limited to within a threshold value of 100μm by inherent crack control in SHCC (Weimann & Li 2003) confirms the potential of SHCC for durable structures.

To enable sound application of SHCC, design models are required, which should eventually be incorporated in standards for structural design with this construction material. Such models do not yet exist, and the pool of experimental data is limited relative to traditional construction materials like reinforced concrete and structural steel. It is argued that computational models, in combination with physical experiments, are effective in developing insight in the behaviour of structures manufactured of such a new material, thereby assisting in the formulation of simpler design models. Such computational models should capture the main mechanisms of behaviour with reasonable accuracy to be objective and allow prediction of structural behaviour beyond that tested in physical experiments.

While detailed micro-models may prove more accurate by capturing interaction of the heterogeneities in SHCC (fibres, hcp matrix, fibre-matrix interfaces), so-called macro-models are pragmatic and allow viable analysis and prediction of structural behaviour.

In this paper a macro-model based on continuum plasticity is proposed and elaborated. Such a model does not distinguish between the various ingredients in SHCC, but considers it to be a homogeneous continuum.

The use of such continuum models for concrete or other cement-based material have become standard in research environments and are even available in commercial finite element packages such as DIANA (2008), which is used in this research.

However, a computational macro-model appropriate for SHCC does not yet exist commercially. A model based on continuum damage was proposed recently by Boshoff & van Zijl (2007),

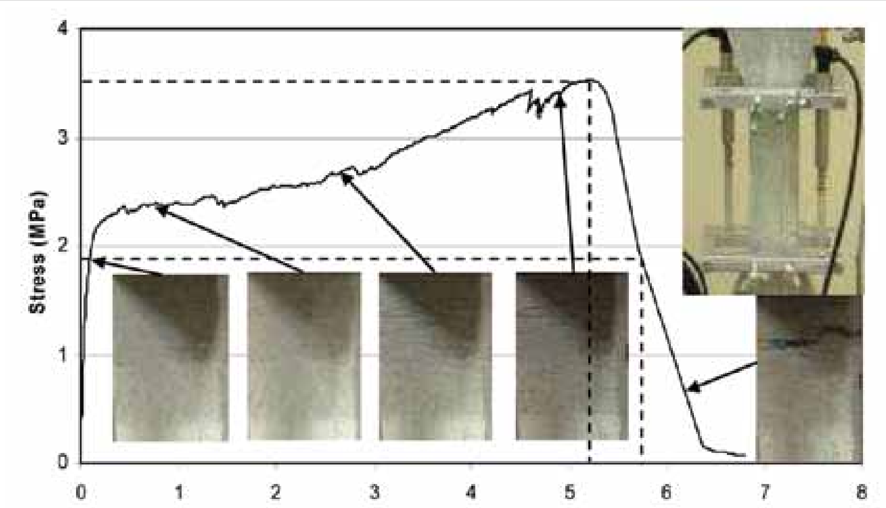

Figure 2: Typical tensile behaviour of SHCC.

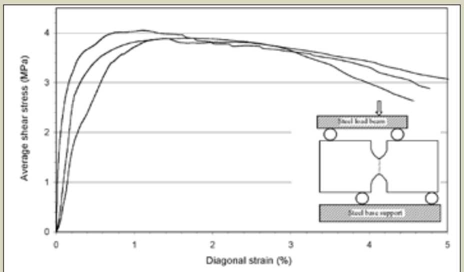

Figure 3: Shear response of SHCC under pure shear (Shang &van Zijl 2007).

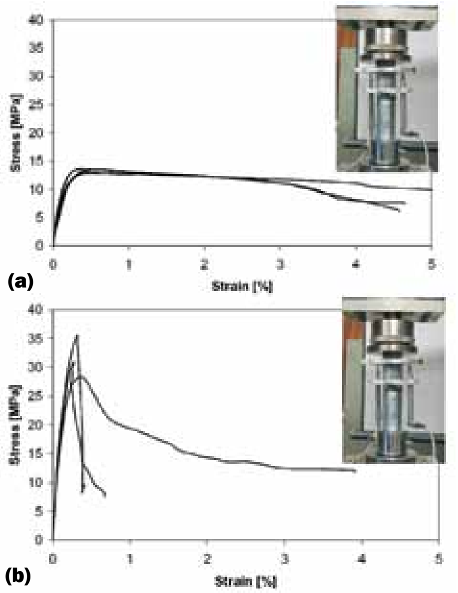

Figure 4: Compression test response of SHCC cylinder specimen 100 mm x 50 mm diameter produced by (a) casting (W/B = 0.4) and (b) extrusion (W/B = 0.25)

but provided for non-linear behaviour in only the tensile regime.

Also, reported SHCC response to cyclic loading (Boshoff 2007, Jun & Mechtcherine 2007) indicates that elastic unloading, as used in a plasticity approach, is more appropriate for SHCC than the secant unloading used in the damage approach. Typical unloading-reloading behaviour is shown schematically in *Figure 1*.

Kabele (2002) also proposed a continuum model for SHCC. This model is limited to tensile non-linearity, and static behaviour, ie time-dependence is not incorporated. The unloading behaviour is elastic in the strain-hardening tensile regime, but secant beyond the peak tensile resistance.

In this paper, a continuum model is proposed for both tensile and compressive behaviour, in terms of a multi-surface continuum plasticity model. Anisotropy is considered in terms of different strengths and hardening-softening responses in orthogonal directions. This has been shown to be relevant for certain manufacturing processes, for instance extrusion, which predominantly

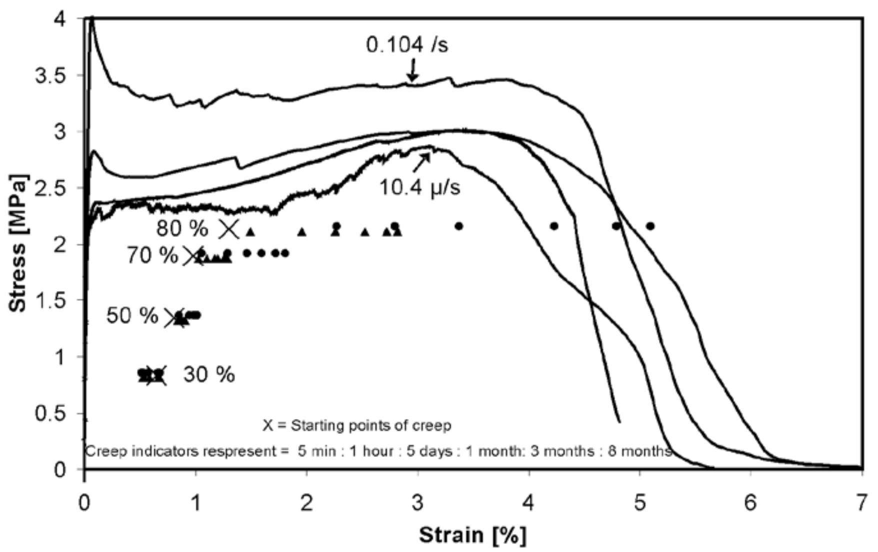

Figure 5: Tensile stress-strain response to tensile tests at various loading rates, and creep tests of pre-cracked specimens at various sustained load levels.

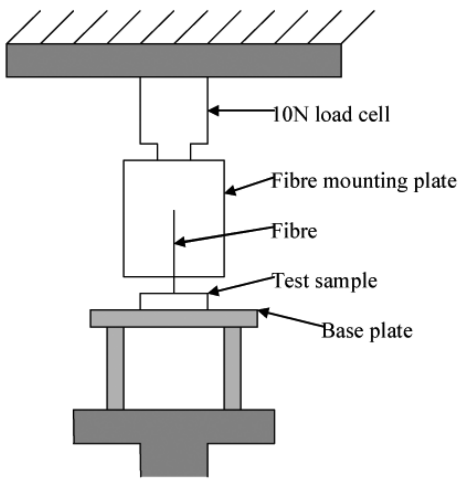

Figure 6

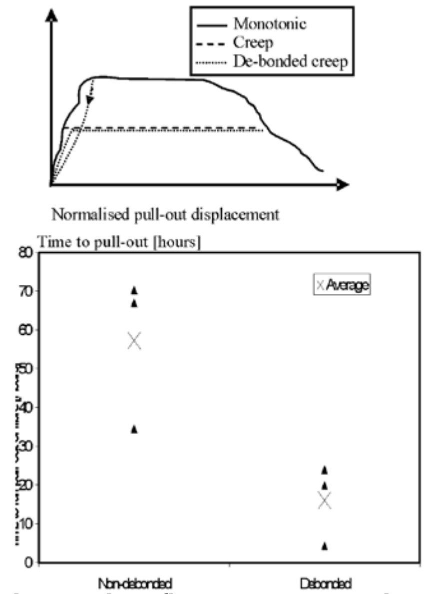

Figure 7: Single fibre creep tests showing (left) the load-deformation and (right) the times to failure (Boshoff 2007).

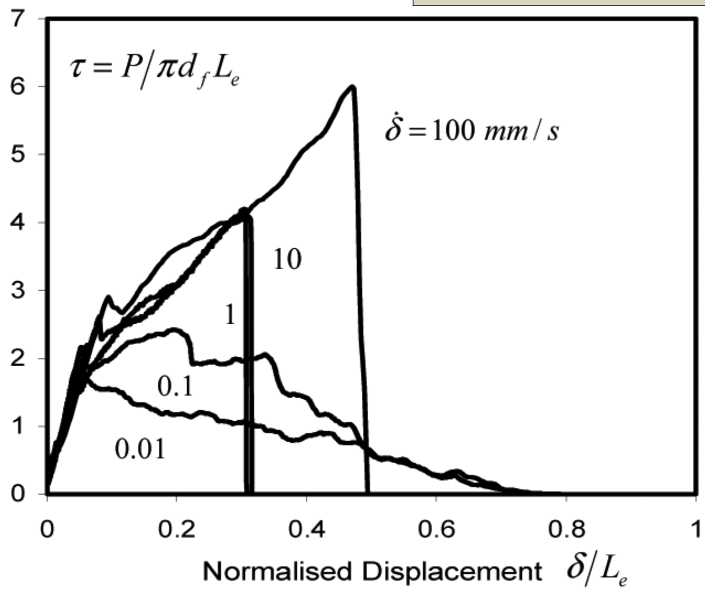

Figure 6: Single fibre pull-out rate tests (Boshoff 2007).

orientates fibres in the extrusion direction. Creep is incorporated in the form of visco-elasticity. In tension, cracking rate-dependence is considered, based on experimental evidence.

2 MECHANICAL BEHAVIOUR OF SHCC

Typical SHCC mechanical behaviour is demonstrated here by results of characterisation tests on a particular SHCC with mix proportions given in *Table 1*, used for all results reported in this paper, unless stated otherwise.

The specimens were produced by normal casting in steel moulds, stripping after two days and curing to an age of 14 days in water at controlled temperature of 23°C. The evolutions of mechanical properties (7 days to 28 days, wet curing) have been reported before (van Zijl 2005). The tensile results here are for thin dumbbell specimens, shown in *Figure 2*, with typical thickness of 15 mm. Compressive results are however for 50 mm diameter cylinders of height 100 mm.

The strain-hardening response of SHCC is associated with multiple crack formation once the tensile strength of the matrix is exceeded. This is shown for a typical case in *Figure 2*.

Instead of significant widening of the first crack, which initiates once the matrix strength is exceeded, more cracks arise upon further deformation. The crack control is a dominant feature of SHCC and holds the key to understanding and predicting its short and long term behaviour.

Through balanced properties of the cement matrix, fibres and their interfaces, based on consideration of micro-mechanical mechanisms (Li *et al*. 1995), pseudo strain-hardening tensile behaviour is achieved.

The conditions for pseudo strain-hardening are well understood and the data base of experimental results towards confirming micromechanical design models is growing.

The ductility of SHCC is shown to exist also under pure shear (*Figure 3*) and uniaxial compression (*Figure 4a*).

Note that the SHCC produced by extrusion (*Figure 4b*) has significantly higher uniaxial compressive strength, due to the lower W/B ratio used to obtain extrudable SHCC, but also due to the high pressure extrusion process and fibre alignment in the extrusion direction.

This high strength is seen to be followed by a steep post-peak reduction in

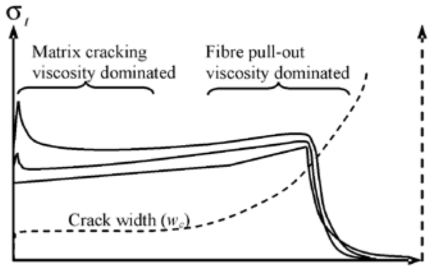

Figure 8: Trends in macroscopic tensile behaviour and mechanisms of rate-dependence.

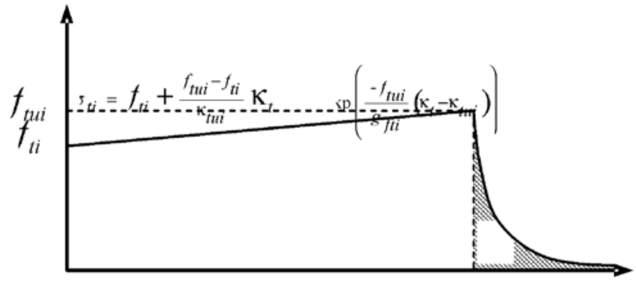

Figure 9: Tensile material law for SHCC.

compressive resistance. The responses of cast SHCC suggest the use of ductile strain-hardening-softening relations to describe the stress-strain responses.

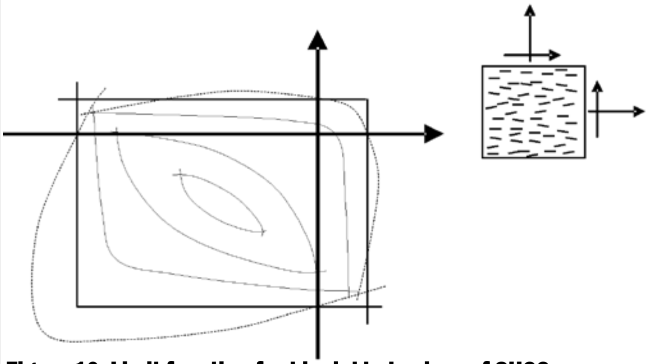

Figure 10: Limit function for biaxial behaviour of SHCC.

3 TIME DEPENDENT BEHAVIOUR OF SHCC

To illustrate the time dependent behaviour of SHCC under mechanical load, results of recent characterizing creep and rate-dependent tensile tests are summarised here. Tests were performed on macro-level as well as on single fibre pull-out level. For the macro tests, the same dumbbell-shaped specimens as in the previous section were prepared and tested. In addition, single fibre pull-out tests were performed. These specimens were prepared with the same matrix, but with a single fibre embedded to a pre-determined embedment length L_e. A series of tests were performed on specimens with different embedment lengths to establish a length suitable for subsequent test series at various pull-out rates, as well as under sustained load. From the initial test series L_e = 1.4 mm was chosen for the rate and creep tests. See Boshoff (2007) for complete details.

3.1 Rate dependence

3.1.1 Rate-dependent response of SHCC composite

Stress-strain responses of a series of tensile rate tests over 4 orders of average strain rate magnitudes $(10^{-5} \le \dot{\varepsilon} \le 10^{-1} s^{-1})$ are shown by the solid lines in *Figure 5*. The first cracking strength appears to be significantly rate-dependent, but the ultimate tensile strength and strain to a lesser degree.

3.1.2 Single fibre pull-out rate dependence

To study the rate effect on the micro-level, single fibre pull-out tests were performed (Boshoff 2007) at pull-out displacement rates over 4 orders of magnitude $(10^{-2} \le \dot{\delta} \le 10^{-2}\ mm/s)$. Typical results are shown in *Figure 6*. A significant increase in peak pull-out force is seen with increased loading rate. At low rates, fibres pull out of the matrix completely, indicated by the gradual reduced resistance beyond the peak in *Figure 6*. Higher rates lead to fibre breakage, followed by an abrupt drop in resistance.

Thus it appears that fibre pull-out rate-dependence is an important mechanism of rate-dependence of the composite material.

3.2 Tensile creep response

The reduced stiffness and resistance of cement-based composites under long term sustained load are well described in the literature (eg. Rüsch 1960, Zhou 1992). This has recently been studied for SHCC in tension by Boshoff (2007). Two series of tests were performed.

3.2.1 Macro creep

Firstly, creep tests of previously undamaged specimens were performed at 50% of the ultimate tensile strength. Secondly, a series of creep tests was performed at various load levels (30%, 50%, 70% and 80% of average peak strength). Note that all the specimens of the second series were pre-cracked by deformation controlled tensile loading to a predetermined tensile strain of 1%. After this preload the specimens were unloaded and subsequently reloaded to the creep load, sustained for a period of eight months. The specimens were kept in a constant environment of 23±1 °C and 65%±5% RH. Two specimens were tested at each load level. The creep strain of the uncracked creep specimens at 50% of peak strength was in the order of 0.15% after 8 months. This is negligible relative to that of the pre-cracked specimens shown in *Figure 5*.

Note that the reduced stiffness is due to the pre-cracking.

After eight months no specimens failed, despite the quasi-static load-deformation/stress-strain envelope being exceeded in the case of the highest (80%) sustained load. Due to the sealant, cracks and spacing could not be observed or measured accurately.

However, individual cracks which existed at the onset of sustained loading were observed to widen in time. Instantaneous jumps in the time dependent deformation graphs provide evidence of new cracks initiating under the sustained load (Boshoff 2007). Both these two sources of time-dependent deformation were confirmed by creep tests performed by Jun & Mechtcherine (2007) and Boshoff *et al*. (2008).

3.2.2 Single fibre pull-out creep

Single fibre pull-out creep tests were also performed to study this important mechanism of creep in the composite. A sustained load causing a bond stress between the fibre and the matrix equalling τ = 1.2 *MPa* was applied, reached by an initial pull-out rate of 1 mm/s. Note that this represents an average normal fibre stress of roughly 1.6 times the average fibre stress in the composite at 80% of the peak load (composite average stress 2.1 MPa). If a correction is made for the random 2D fibre orientation, whereby fewer fibres effectively bridge the crack, but at higher stress, the single fibre sustained load is representative of the composite situation. In a first series the fibre in each specimen was initially de-bonded by loading the fibre to just beyond τ_0 and then unloading, before commencing with the creep test. τ_0 is the average bond stress which marks the end of the linear load pull-out response. In a second series of three specimens, the test was performed on the undamaged (non de-bonded) specimen. In *Figure 7* the creep tests and resulting times to complete pull-out, or failure, are shown.

To distinguish fibre creep from the pull-out creep deformation, the time-dependent deformation of a single fibre was measured under a sustained normal stress of 580 MPa. This creep load is nearly five times the fibre normal stress in the pull-out creep stress.

Under these conditions insignificant time-dependent deformation of the fibre was measured. Thus, time dependent fibre pull-out appears to be an important mechanism of creep in the composite material.

3.2.3 Creep mechanisms

From the previous sections the main mechanisms of creep are identified as (i) the initiation of new cracks under sustained load, (ii) widening of cracks due to fibre pull-out, (iii) matrix creep. It was shown for the particular fibre that a potential fourth mechanism, namely fibre creep, does not contribute to creep in the SHCC studied here. It was also noted in section 3.2.1 that the uncracked matrix creep is small relative to the time-dependent deformation of cracked specimens, which implies that the mechanisms of crack initiation and widening due to fibre pull-out dominate.

To interpret these creep mechanisms, it is useful to study the trends in macroscopic tensile behaviour (*Figure 5*), in close connection with the micro behaviour of individual fibre pull-out (*Figures 6 and 7*), as well as micro-crack formation. The result of such scrutiny is presented as a schematised postulation in Figure 8. Also shown in this schematic figure as a dashed line is the crack width development, based on results reported by Boshoff *et al*. 2008. Cracks are controlled to small widths (in the range 50-150μm) over a large tensile deformation range. Such small crack widths imply that the lengths of fibres pulled out at the positions of cracks are also this small. This means that fibre pull-out cannot be the mechanism in the early strain-hardening stages, because the rate-enhanced resistance is mobilised at larger pull-out lengths, apparent from *Figure 6*. Only once the crack width increases, ie towards the end of the strain-hardening regime in *Figure 8*, this mechanism is activated.

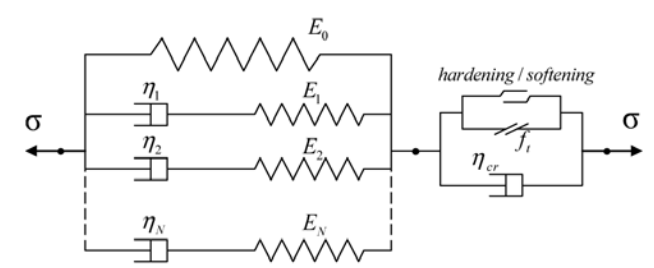

Figure 11: Schematic representation of the constitutive model.

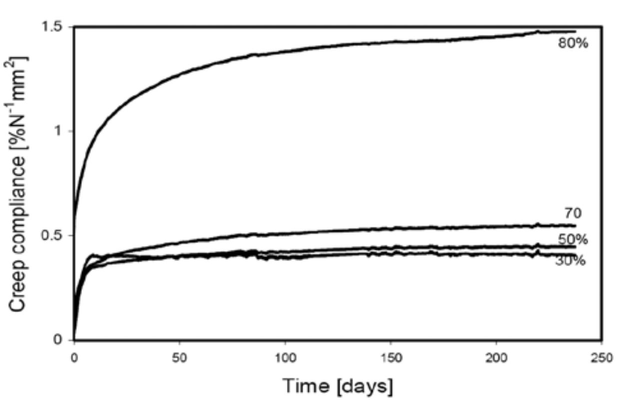

Figure 12: Tensile creep compliance measured on dumbbell SHCC specimens.

The initial rate-dependence is ascribed primarily to matrix cracking viscosity (Zhou 1992, Wu & Bažant 1993, van Zijl *et al*. 2001).

4 MODELLING OF SHCC TIME-DEPENDENT BEHAVIOUR

4.1 Computational framework

A continuum approach is followed. It is assumed that the tensile load-deformational behaviour measured over a practical gauge length on small specimens, for instance 80 mm on the dumbbell shown in *Figure 2*, is simply translated to stress-strain behaviour. *Figure 9* shows the assumed tensile material law, including a linear hardening and exponential softening tensile stress (σ_{ti}) - equivalent strain (κ_t) relation. The softening is controlled by fracture energy (g_{fti}). Note that the subscript i denotes the two material directions x and y respectively.

Anisotropy, which may be significant due to particular manufacturing processes, is considered. For instance, in extruded products dominant fibre orientation in the extrusion direction have been shown to cause flexural strength in the extrusion direction of roughly 2.5 times that in the orthogonal direction (Visser & van Zijl 2007). To account for such lower strength in the orthogonal direction, the same basic shaped stress-strain law as in *Figure 9* is used for tension in that direction, but with different values for first cracking stress (f_{ty}), ultimate tensile stress (f_{tuy}), strain at ultimate stress (κ_{tuy}), and fracture energy (g_{ty}), than those for the main material direction (f_{tx}, f_{tux}, κ_{tux} g_{tx}).

No test results for biaxial behaviour SHCC are available yet, with a test program for such behaviour currently in progress at the University of Stellenbosch. However, shear test results (Li *et al*. 1994, van Zijl 2007) indicate that SHCC shear resistance exceeds its uniaxial tensile resistance. Mechanisms include fibre confinement by compression orthogonal to the diagonal shear cracks, as well as steeper crack alignment to mobilise greater compressive resistance, enabled by retained tensile resistance beyond first cracking. These results imply non-trivial biaxial behaviour of SHCC, eg as shown by the dashed lines in *Figure 10*. For lack of sufficient characterising data, the solid line limit functions in *Figure 10* are assumed for the current computational framework.

Note that a plane stress state is considered and shown in *Figure 10* in terms of the two orthogonal normal stresses. This is appropriate for the thin-walled SHCC specimens used here.

Also shown in *Figure 10* are the limit functions for compression, which are also taken as simple straight lines in the zero shear stress (principal stress) plane. Similar expressions are used for the compressive stress-strain responses as for the tensile stress-strain model shown in *Figure 9*, with parameters f_{cx}, f_{cux}, κ_{cux}, g_{cx} and f_{cy}, f_{cuy}, κ_{cux}, g_{cy} respectively.

This is used for simplicity, but improved resemblance with the measured compressive responses - for example those in *Figure 4* - can easily be obtained by defining alternative hardening-softening curves, for instance parabolic hardening and linear softening.

4.2 Constitutive model for SHCC

In a plane stress setting with stress and strain vectors

$$\sigma^T = \lfloor \sigma_x \sigma_y \tau \rfloor,\ \varepsilon^T = \lfloor \varepsilon_x \varepsilon_y \gamma \rfloor \quad (1)$$

the material law can be expressed as follows

$$\dot{\sigma} = D^{ve}\,\dot{\varepsilon}^{ve} + \Sigma = D^{ve}\left(\dot{\varepsilon} - \dot{\varepsilon}^p\,\dot{\varepsilon}^o\right) + \Sigma \quad (2)$$

where $\mathbf{D}^{ve}$ is an equivalent time-dependent stiffness modulus, $\dot{\varepsilon}^{ve}$, $\dot{\varepsilon}^p$ and $\dot{\varepsilon}^o$ are the visco-elastic, plastic and initial strain vector respectively and Σ is a viscous stress vector accounting for the history. Full detail of the computational treatment is given by van Zijl *et al.* (2001). There it is shown that the visco-elastic stiffness is computed from the spring stiffnesses (E_i) and dashpot viscosities (η_i) of the elements in the Maxwell chain shown in *Figure 11*. The stress history term accumulates the stresses in each chain element at the end of the previous time step. Linear time integration is used to integrate eq. (2).

To incorporate the various sources of time dependence, the limit functions and their evolutions according to the hardening-softening shown in *Figure 9* are enhanced by consideration of bulk visco-elasticity through the Maxwell-chain, as well as cracking viscosity (η_{cr}), as schematised in *Figure 11*. Note that the latter is activated only in tension.

The limit stresses are treated in multi-surface plasticity fashion, whereby the plastic strain increment is expressed as follows:

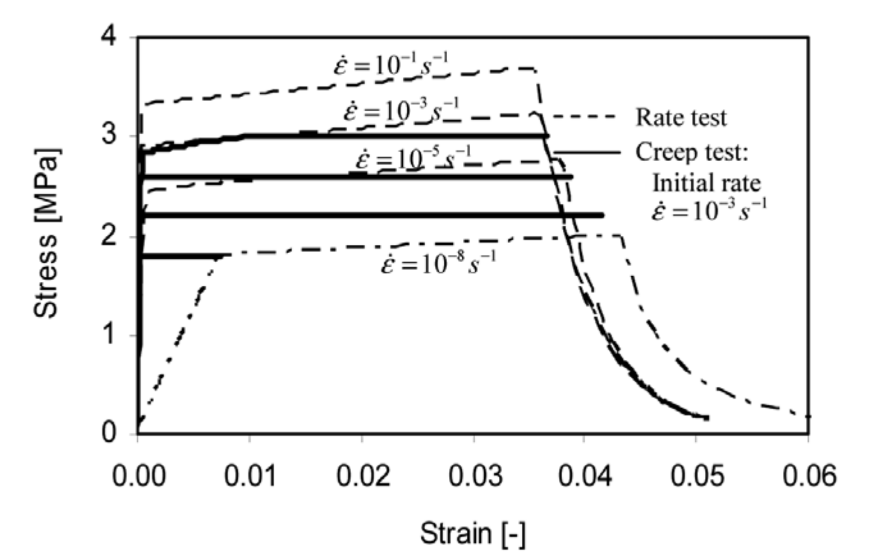

Figure 13: Computed rate and creep responses of SHCC.

$$\Delta\varepsilon^p = \Delta\lambda \frac{\partial f}{\partial \sigma} \quad (3)$$

with λ the amount of plastic flow/crack strain and *f* the flow function. For tension, the anisotropic Rankine yield function is chosen (represented by the solid line in *Figure 10*), which is a maximum principal stress failure criterion, formulated as

$$f_t = \frac{(\sigma_x - \sigma_{tx}) + (\sigma_y - \sigma_{ty})}{2} + \sqrt{\left(\frac{(\sigma_x - \sigma_{tx}) + (\sigma_y - \sigma_{ty})}{2}\right)^2 + \alpha_t \tau^2} \quad (4)$$

The current admissible stresses in the material x, y directions are denoted by σ_{tx} and σ_{ty} respectively.

Simple expressions for the tensile resistance are given in *Figure 9*. As stated in the previous section, separate expressions are used in the orthogonal directions, with separate sets of model parameters. The hardening-softening is governed by equivalent tensile strain K_t, with an appropriate measure for SHCC considered to be the maximum principal plastic strain given by

$$\kappa_t = \dot{\varepsilon}_1^p = \frac{\dot{\varepsilon}_x^p + \dot{\varepsilon}_y^p}{2} + \sqrt{\left(\frac{\dot{\varepsilon}_x^p - \dot{\varepsilon}_y^p}{2}\right)^2 + \left(\frac{\gamma}{2}\right)^2} \quad (5)$$

The equivalent strain increment can be shown to be directly related to the plastic flow increment ($\Delta K_t = \Delta\lambda_t$) insert symbols. The parameter α_t controls the shear contribution to tensile failure.

In compression, the limit function is

$$f_c = -\frac{(\sigma_x - \sigma_{cx}) + (\sigma_y - \sigma_{cy})}{2} + \sqrt{\left(\frac{(\sigma_x - \sigma_{cx}) + (\sigma_y - \sigma_{cy})}{2}\right)^2 + \alpha_c \tau^2} \quad (6)$$

The equivalent compressive strain is

$$K_c = \varepsilon_2^p = \frac{\varepsilon_x^p + \varepsilon_y^p}{2} + \sqrt{\left(\frac{\varepsilon_x^p - \varepsilon_y^p}{2}\right)^2 + \left(\frac{\gamma}{2}\right)^2} \quad (7)$$

As for tension, it can be shown that the $\Delta K_c = \Delta\lambda_c$.

The intersection between the two limit surfaces is treated in a consistent way, as proposed by Koiter (1953).

$$\Delta\varepsilon^p = \Delta\lambda_t \frac{\partial f_t}{\partial \sigma} + \Delta\lambda_c \frac{\partial f_c}{\partial \sigma} \quad (8)$$

In tension, a cracking rate-dependence is introduced following Wu & Bažant (1993) and van Zijl *et al.* (2001) as follows:

$$\Delta w = \Delta w_r \sinh\left[\frac{\sigma - \sigma_t(w)}{c_1\left[\sigma_t(w) + c_2 f_t\right]}\right] \quad (9)$$

where $\dot{w}_r$ is a constant, reference crack opening rate.

The crack width *w*, which is assumed to be spread uniformly across the fracture process zone of width l_b, can be related to the equivalent strain as follows:

$$K_t = {}^{w}\!/_{l_b} \quad (10)$$

With eqs. (9, 10) the tensile strength equations (*Figure 9*) can be rewritten as

$$\sigma_{ti} = \left(f_{ti} + \frac{f_{tui} - f_{ti}}{K_{tui}} K_t\right) \quad \forall \quad K_t \le K_{tui} \quad (11)$$
$$\left[1 + c_t \sinh^{-1}\left(\frac{\dot{K}_t}{\dot{K}_r}\right)\right] + c_1 c_2 f_{tui} \sinh^{-1}\left(\frac{\dot{K}_t}{\dot{K}_r}\right)$$

$$\sigma_{ti} = f_{tui}\exp\left(\frac{-f_{tui}}{G_{fti}/l_b}(K_t - K_{tui})\right) \forall \quad K_t > K_{tui} \quad (12)$$
$$\left[1 + c_t \sinh^{-1}\left(\frac{\dot{K}_t}{\dot{K}_r}\right)\right] + c_1 c_2 f_{tui} \sinh^{-1}\left(\frac{\dot{K}_t}{\dot{K}r}\right)$$

where the index i refers to the materials axes. The coefficient c_2 is a small offset value to prevent singularity of eq. (9). The reference strain $\dot{K}_r$ rate is directly related to $\dot{w}_r$ cf. eq. (10).

It should be a sufficiently low cracking rate at which the cracking strengths are rate-independent. In the current model, the rate terms represent all physical processes causing rate dependence, including both cracking viscosity and fibre pull-out rate-dependence. The constitutive model has been implemented as a user material in DIANA (2008).

5 MODELLING RATE DEPENDENCE AND CREEP FRACTURE

The ability of the model to represent observed SHCC rate-dependence and creep is demonstrated in this section. The simple case of uniaxial tension is considered here, representing the case for which the results are shown in *Figure 5*. The model parameters were taken as average values of the following test results:

(i) Monotonic, uniaxial tensile tests at low rates on dumbbell specimens to obtain the quasi-static tensile strength and hardening-softening parameters.

Note however that the lowest physical test load rate of $\dot{\varepsilon} = 10^{-5}\, s^{-1}$ was used. To incorporate lower tensile resistance at an even lower rate, the reduced values f_{tx} = 1.8 MPa, f_{tux} = 2.0 MPa, K_{tux} = 0.035 and g_{tx} = 0.01 N.mm^{-2} were chosen by inverse analysis to represent the case for $\dot{\varepsilon} = \dot{K}_r = 10^{-8} s^{-1}$.

(ii) Tensile creep tests on dumbbell specimens to compute spring stiffness and dashpost viscosities in the linear visco-elastic range, ie up to 50% of peak load – *Figure 12* shows that tensile creep loads beyond 50% lead to nonlinear creep. Note that shrinkage has been measured on separate specimens and has been compensated for.

(iii) Rate-dependent tensile tests on dumbbell specimens, from which the cracking rate model (eqs. 11, 12) parameters were computed by inverse analysis:

$$c_1 = 0.05, c_2 = 0.001 \; and \; \dot{K}_r = 10^{-8}\, s^{-1}$$

The finite element model results computed with the constitutive model are presented in *Figure 13*. The numerical results of rate-dependent tensile tests are shown in dashed lines, with tensile strain rates coinciding with those in the physical experiments (*Figure 5*).

Also shown in the figure are numerical results of tensile creep analyses at various levels of sustained load (1.8, 2.4, 2.8 and 3.2 MPa). The results indicate that the creep limit is reached for tensile creep at a sustained load level below a certain threshold, in this case 2 MPa. Delayed fracture of the specimen does not occur at loads below this level. Beyond this level, creep fracture occurs after significant creep deformation. This is in agreement with the experimental results for the case of 80% sustained load in *Figure 5*, except that the physical specimens have not yet fractured. Nevertheless, delayed fracture is expected, based on reported creep fracture at high sustained tensile load (Jun & Mechtcherine 2007) and observed in tensile creep tests on notched SHCC specimens (Boshoff *et al*. 2008).

Note further that the computed responses to the rate-dependent, monotonic tests form an envelope of deformability for the creep specimens, beyond which creep fracture occurs.

The numerical results shown in *Figure 13* are in reasonable agreement with the measured responses in *Figure 5*. Note however, that no attempt was made to incorporate a strain-dependent rate term to simulate the different mechanisms of rate-dependence described in section 3.2.3. By such distinction, improved agreement with experimental results may be obtained.

6 CONCLUSIONS

This paper proposes a constitutive model for SHCC. Mechanisms of tensile creep and rate-dependence have been identified from recent experimental results. Rate-dependence of the cement-based matrix is considered to dominate in the low deformation range after first cracking, while rate-dependent fibre pull-out governs the response at large deformations.

The constitutive model incorporates anisotropy in terms of different strengths and strain-hardening-softening curves for orthogonal material directions, for both tension and compression. The framework of multi-surface continuum plasticity is used and extended to incorporate visco-elasticity for the bulk creep and cracking rate-dependence.

The model requires further characterisation for biaxial loading. For lack of such data, simple Rankine-type limit functions have been suggested and elaborated here. Current research activities include biaxial testing of SHCC to investigate whether the linear functions are appropriate.

The model has been implemented as a user material in a commercial finite element programme and used in finite element analyses to demonstrate its ability to capture the phenomena of creep, creep fracture and rate-dependence with reasonable accuracy.

However, the model does not distinguish between the identified different physical mechanisms of rate-dependence, acting at different levels of deformation in SHCC. This is a continued research focus.

ACKNOWLEDGEMENTS

This research has been performed under the THRIP project SAPERCS. The Department of Trade and Industry and the industry partners of this project, namely Infraset, the Cement and Concrete Institute, Grinaker-LTA, Africon, BKS, Element Consulting Engineers are gratefully acknowledged.

Ingredient materials were generously donated by PPC (cement), Chryso South Africa (chemical additives) and Kuraray Japan (PVA fibres).

The research results of Heinrich Stander (MScEng, 2007), Christo Visser (MScEng, 2007) and Dr Billy Boshoff (PhD, 2007) at Stellenbosch University have been invaluable in this work.

REFERENCES

1. Bažant, Z P, and Najjar, L J 1971. Drying of Concrete as a Non-Linear Diffusion Problem, Cement and Concrete Research 1, pp. 461-473.
2. Boshoff, W P 2007. Time-dependant behaviour of ECC, PhD dissertation, Stellenbosch University, South Africa.
3. Boshoff, W P Adendorff, C and GPAG van Zijl, 2008. Creep of Cracked Strain-Hardening Cement-based Composites, CONCREEP8, Sept 2008, Tokyo.
4. Boshoff W P and van Zijl, G P A G 2007. A computational model for strain-hardening fibre-reinforced cement-based composites. J SAICE, 49(2) 24-31.
5. DIANA v 9.3, 2008. DIANA Users Manual, TNO DIANA BV, Delft, The Netherlands.
6. Jun, P and Mechtcherine, V. 2007. Behaviour of SHCC under repeated tensile loading, RILEM PRO 53: HPFRCC5, Mainz, Germany pp. 97-104.
7. Kabele, P 2002. Equivalent continuum model of multiple cracking, Engng. Fracture Mechanics, 9(1/2), pp. 75-90.
8. Koiter, W T 1953. Stress-strain relations, uniqueness and variational theorems for elastic-plastic materials with singular yield surface, Q. Appl. Math. 11(3), pp. 350-354.
9. Lepech, M and Li, V. C. 2005. Water

REFERENCES continued

Permeability of Cracked Cementitious Composites, Proceedings of ICF11, Turin, Italy, Mar. 2005, pp. 113-130.

10. Li, V C Mishra, D K Wu, H.C. 1995. Matrix design for pseudo strain-hardening FRCC, Materials and Structures, 28, pp. 586-595.
11. Li, V C, Mishra, D K, Naaman, A E, Wigh, J K, LaFave, J M, Wu, H C and Inada, Y, 1994. On the shear behavior of engineered cementitious composites, Journal of Advanced Cement Based Materials 1 (3), pp. 142–149.
12. Neithalath, N 2006. Analysis of Moisture Transport in Mortars and Concrete using Sorption-Diffusion Approach, ACI Materials J. 103(3), 209-217.
13. Rapoport, J, Aldea C, Shah, S P, Ankenman, B and Karr, A F 2001. Permeability of Cracked Steel Fibre-Reinforced Concrete. Technical Report Number 115, January, 2001, National Institute of Statistical Sciences.
14. Rüsch, H 1960. Researches toward a general flexural theory for structural concrete, ACI J. 57(1), pp. 1-28.
15. Sahmaran, M, M Li, and V C Li 2007. Transport Properties of Engineered Cementitious Composites Under Chloride Exposure, ACI Materials J. 104(6), 604-611.
16. Shang Q J and van Zijl G P A G. (2007). Characterising the shear behaviour of SHCC. J SAICE, 49(2) 16-23.
17. Van Zijl, G P A G 2005. The role of aggregate in high performance fibre-reinforced cement-based composites. Concrete Beton, Nr 110, September 2005, pp. 7-13.
18. Van Zijl, G P A G 2007. Improved mechanical performance: Shear behaviour of strain hardening cement-based composites (SHCC). Cem. and Concr. Res., 37(8), pp. 1241-1247.
19. Van Zijl, G P A G. 2008. Durability of strain-hardening cement composites (SHCC) – an overview, CDROM Proc. ICCRRR, Nov 2008, Cape Town.
20. Van Zijl, G P A G, de Borst, R and Rots, J G (2001). The role of crack rate dependence in the long-term behaviour of cementitious materials. Int. J. Solids and Structures, 38(30-31), pp. 5063-5079.
21. Visser, C R and van Zijl, G P A G 2007. Mechanical characterisation of extruded SHCC, RILEM PRO 53: HPFRCC5, Mainz, Germany pp. 165-173.
22. Wang, K, Jansen, D C, Shah, S, and Karr, A F 1997. Permeability study of cracked concrete, Cement and Concrete Research, 27(3) 381-393, 1997.
23. Weimann, M B and Li, V C 2003. Hygral Behavior of Engineered Cementitious Composites (ECC), International Journal for Restoration of Buildings and Monuments 9(5), 513–534.
24. Wu, Z S and Bažant, Z P 1993. Finite element modelling of rate effect in concrete fracture with influence of creep, Creep and Shrinkage of Concrete (eds. Z P Bažant and I.Carol), E.&F.N.Spon, London, pp. 427-432.
25. Zhou, F P 1992, "Time-dependent Crack Growth and Fracture in Concrete," PhD thesis, University of Lund, Sweden.

Crowds flock to the Concrete Boat Race

Inland's Concrete Boat Race

The Inland Branch held their 20th Annual Concrete Boat Race Day at the Victoria Lake Club in Germiston, near Johannesburg in September. Each year sees an improvement in the event and this year was no exception, with 70 boats taking to the water and well over 1 000 supporters cheering the rowing team of their choice.

The day attracted a record number of participating companies and in his closing remarks, the Inland Branch Chairman, John Sheath thanked the organising committee, the industry, sponsors, lecturers and students for their continuing support of this now prestigious event on the Inland Branch calendar.

Support from the local universities was excellent, and as in the past, some had included the boat construction in their student syllabus as a project management exercise. Success on the day was due largely to the support from industry representatives who provided financial and other support. Special thanks therefore go to the following companies/organisations: AfriSam, Ash Resources, BASF Construction Chemicals, Basil Read, Blitz Beton, Cement and Concrete Institute, Chryso SA, Group 5, Infraset, Lafarge SA, PPC Cement, Rocla and WR Grace.

Special prizes - compliments of PPC Cement - were awarded to Deon Kruger for the lecturer who registered the largest number of boats on behalf of the University of Johannesburg and for the greatest increase in the number of boats and students compared to the event in 2008.

The judges: Colin Kalis and Hanlie Turner

There was a new prize on offer this year which was awarded to the first boat that sank. This occurred in 10 seconds from the start of the first race and went to the head of the engineering department at one of the universities. The name has been withheld to protect the team's reputation.

The prize (a concrete boot) was sponsored and presented by Modcon Precast of Johannesburg.


Some struggled to make the course

	Boat Name	Team of PPC Cement)	Prize (compliments
STUDENT CONSTRUCTION			
1ST	FLYASH	University of Johannesburg	R6,000
2ND	ARK	University of Johannesburg	R2,500
3RD	GO GREEN	Tshwane University of Technology	R1,000
SPECIAL MENTION	QUEEN MARY	University of Johannesburg	-

Category and Position	Boat Name	Team
STUDENTS RACE		
1ST	Viermaneenroeispaanangedrewerbetonwater-vervoermiddel	University of Pretoria
2ND	Crafty	University of Johannesburg
3RD	Wet 'n Wild	University of Johannesburg
INDUSTRY RACE		
1ST	PPC Hercules	PPC Cement
2ND	DuraPozz	Ash Resources
3RD	Rocla Racoon	Rocla
LADIES RACE		
1ST	PPC Sales/Marketing 2	PPC Cement
2ND	The Submarine	Group 5
3RD	Rocla Racoon	Rocla

Gillooly's Interchange

The site visit to Gillooly's Interchange, one of the busiest interchanges in South Africa was one of the unique events members attended recently. The Gauteng Freeway Improvement Project (GFIP) incrementally launched the bridge at Gillooly's Interchange, where the N3 and N12 meet, to the east of Johannesburg. More than 50 enthusiasts, ranging from consulting engineers and contractors, to suppliers and academics, were hosted on this special visit by the main contractor, CMC di Ravenna South Africa.

The afternoon began with a detailed presentation by a visiting CMC engineer from Italy on all aspects of the bridge

construction covering design, logistics, erection and launching. In summary this part of the project, named Work Package I is the final GFIP project in the first phase, entailing the upgrade of 10km of the N12 between the N3 (Gillooly's) and the R21 interchanges, as well as the N3 section between the N12 and Modderfontein interchanges. The consultants for this section are Gillooly's Joint Venture and the main contractor is CMC/G4 Joint Venture.

A highlight is the construction of a 200m-long, incrementally launched bridge designed to relieve the weaving action of traffic within the Gillooly's Interchange. The curved bridge is being cast in increments, from the Boksburg side, and will take the Boksburg to Sandton traffic movement.

Unique to Work Package I is the use of an ultra-thin concrete base for the new road sections. The base is heavily reinforced using 50x50x5mm steel mesh, and the concrete itself has a high concentration of steel fibres yielding a strength of approximately 120MPa.

KZN's Egg Protection Device Competition

KZN's Egg Protection Device Competition arranged by the KZN branch and sponsored by NPC Cimpor was well attended with 23 student entries and 10 entries from industry. Students from MUT, UKZN and DUT took part in a closely contested competition at the Berea Rover Sports Club. The teams got to see whose concrete arch could take the most blows from an overhead weight before the arch cracked and broke the egg underneath. Participants and supporters showed great enthusiasm and the excitement and noise levels were on a par with last year's event.

The evening was a great success for all parties who participated. NPC Cimpor is proud to be associated with this event and would like to see this event grow from strength to strength in the future. This will remain an important event on the KZN CSSA's calendar.

The winners were awarded their prizes by Laurence Stevens, NPC Cimpor's Operations Manager, who handed over cheques to the winners.

The winner of the Student Competition was Shumbuzo Mngadi from MUT. Second place went to Andrew Maro from UKZN and in third place Silindile Gloria Maphumulo from MUT.

The hotly contested industry competition saw Nishal Surjoo from Lafarge take first place.

First place went to MUT team number 2: Nondumiso Thulile Gumede, Penny Gugu Mbuyisa and Mlungiseni Biyela with Dion Kuter – KZN CSSA Branch Chairman, Rowan Scully – KZN CSSA Committee Member/NPC Cimpor Key Account Manager)

Second place: DUT team: Robert Mc Cann, Bradley Hall, Brent Kloppers and members

Laurence Stevens from NPC Cimpor with Nishal Surjoo from Lafarge take first place. Mthokozisi Themba Shezi from Contest came second, and in third place MA Mncwabe from Lafarge.

The winning students, in first place Shumbuzo Mngadi from MUT, 2nd place was Andrew Maro from UKZN, NPC Cimpor's, Laurence Stevens next to Silindile Gloria Maphumulo from MUT in 3rd place.

Eastern Cape's concrete chatter

The end of the year is rapidly approaching and we are about to bid farewell to an interesting and busy year. The year started off at a sprint with the organisation and hosting of the very successful Self Compacting Concrete (SCC) full day seminar in February as well as the AGM at the end of the same month.

Things certainly did slow down a little in terms of CSSA activities as committee members' work commitments escalated and between the AGM and now we only managed to organise and host the Fulton Awards Dinner at the King Edward Hotel in June, which also was a huge success with approximately 140 people attending. To close off the year, two final events have been arranged: the Concrete Diagnostics and Repair Methods end of October; and the Coega Bridge Site Visit during November. In 2010 the Eastern Cape branch intend hosting a 'Concrete mix design and specification' workshop during March.

Koeberg Interchange site visit

The Koeberg Interchange Phase 1 site visit and project briefing was hosted by Group 5 Civils. The event was well attended and over-subscribed to by engineers, contractors and suppliers.

John Colman briefed the society's delegates on the scope of the work, the project deadlines and the current progress.

After the briefing, the attendees toured the site and discussed construction aspects in detail. They were given first hand knowledge of the operation and the magnitude of the upgrade to the Interchange in the City of Cape Town.The branch is hoping that a second visit will be possible during the second quarter of 2010.

Western's Concrete Cube Competition

The Western Cape Branch held the prize-giving for the annual Concrete Cube Competition at the University of Cape Town's concrete laboratory.

The quest for accuracy continued this year with a target compressive strength challenge set at 90.0 MPa for the 100 mm cube specimens, limiting mass to 2.6 kg but permitting the use of any material.

In recent years the number of entries has increased dramatically due to a higher number of civil engineering students at the academic institutions which also results in tougher competition.

This year was no exception with 43 group entries. Support and attendance from the local universities was great.

Special thanks to Hans Beushausen for conducting the cube tests and hosting the event at UCT.

Special thanks to Doka and their representatives who provided the catering as well as booby prizes.

Mike Otieno with Hans Beushausen

Student results: 1. Mike Otieno (UCT) 90.0 MPa; 2. Simon Braun (UCT) 89.8 MPa; 3. Tony Meri (UCT) 88.6 MPa; Non-student; 1. Charles May (UCT Laboratory) 97.0 MPa

Runner up Simon Braun

Self Compacting Cement

Recognising that some SCC can be almost liquid-like in nature, the American Concrete Institute (ACI) Committee 347, Formwork for Concrete, recommends a very conservative approach to formwork design. The committee suggests that formworks are designed with the assumption that full liquid pressure head will be achieved unless trial study measurements can prove otherwise.

This is because ordinary concrete behaves like a malleable body depending on the slump and temperature, however SCC behaves like a liquid and does not have the ability to support part of its own weight within five hours, therefore resulting in the need for walling systems that can withstand greater pressures for higher casting heights.

In South Africa most contractors and suppliers possess modular systems that can withstand fresh concrete pressures of 60kN/m². With the utilisation of SCC these systems will only be able to realize pour heights of maximum 2,4m. A limited amount of contractors and suppliers are in possession of systems that can withstand pressures of 80kN/m², realizing pour heights of up to 3,2m possible.

For walling and columns' pour heights greater than 3,2m, special formwork solutions will need to be utilised either made of special steel design or of a variable solder/waler application utilising standard components designed to suit the relevant pressure anticipated.

The contractor will need to ensure that the following considerations are in order to ensure successful concreting. Formwork will need to be designed to withstand the relevant concrete pressure. No gaps in shutter to be wider than 2mm and all other gaps to be sealed. Box outs need to be bolted down/ securely fixed and braced

The best way of pouring SCC is to let it flow from one point. It flows up to 20 m horizontally. But having box-outs for doors within these 20m will result in single sided concrete pressure on the box-out, which will destroy it, so pour alternately.

A concrete kicker is advisable to assist with sealing of gaps. Groutex should be utilised. Formwork has to be tied/bolted down to the founding wall below, to prevent upliftment. Watertight chamfers, cones and ferrule tubes are required.

The additional consumables will definitely impose an additional cost to the wall formwork process however the actual formworking material cost and any additional cost can only be realised once the pour height, finish requirement, cycle time and the amount of materials have been determined.

Concrete placement

There are three options for the placement of concrete. Option 1: with watertight concrete skip and a flat hose allows the placement to take place from the bottom. Option 2: Pumped with the discharge pipe placed between rebar to allow the placement to take place from the bottom. (Minimum space between rebar is 140mm). Option 3: with a formwork concrete pump connector to allow the placement to take place from the bottom with a static pump.

Slab formwork

SCC concrete does not impose any additional load onto the slab formwork. The form lining will need to be watertight, resulting in additional cost of consumables. Modular decking systems are questionable and not recommended. Soffits with a fall are not possible without top shutter, resulting in an additional cost.

Special formwork applications

With tunnels, underpinning ,shaped beams and buttress columns, SCC has the obvious advantages over normal concrete placement due to the blind workface and inaccessibility. Special Engineering & Design will be necessary.

References

1. Heiner Lorenz(Dipl.Ing) Product Manager, Peri Formwork & Shoring
2. Riaan Brits(Pr Eng) Sales Engineer, Wiehahn Formwork & Scaffolding
3. Ariane Standt (Dipl.Ing) Design Engineer, Wiehahn Formwork & Scaffolding
4. Sika Concrete Handbook
5. American concrete institute (ACI)

Company Membership Details

Platinum	Principal Member	Address	Tel No	Fax No
NPC-Cimpor (Pty) Ltd	Mr P Strauss	PO Box 15245 Bellair 4006	031 450 4411	086 535 2772
Gold	**Principal Member**	**Address**	**Tel No**	**Fax No**
BKS Engineering & Mangement (Pty) Ltd	Mr PD Ronné	PO Box 112 Bellville 7535	021 950 7500	021 950 7502
Silver	**Principal Member**	**Address**	**Tel No**	**Fax No**
Cement & Concrete Institute	Mr B Perrie	PO Box 168 Halfway House 1685	011 315 0300	011 315 0584
MAPEI	Mr C van der Merwe	PO Box 365 Brakpan 1540	011 876 5336	011 876 5160
Chryso SA (Pty) Ltd	Mr NS Seymore	Postnet Suite 59 Private Bag X1 East Rand 1462	011 395 9700	011 397 6644
Bronze	**Principal Member**	**Address**	**Tel No**	**Fax No**
Shukuma Flooring	Mr A Stücki	PO Box 15552 Emerald Hill 6000	041 372 1933	041 372 1944
Lategan & Bouer Engineers	Mr K Lategan	PO Box 1251 Secunda 2302	017 634 4150	017 634 4188
Scribante Concrete	Mr S Scribante	PO Box 2179 North End 6056	041 484 7211	041 484 6231
Quickslab (Pty) Ltd	Mr J Coetzee	PO Box 9 Brackenfell 7560	021 982 1490	021 982 1492
Empa Structures	Mr CA Bain	PO Box 3846 Durbanville 7551	021 988 8840	021 988 8750
Doka South Africa	Mr U Meyer	PO Box 8337 Halfway House 1685	011 310 9709	011 310 9711
Jeffares & Green (Pty) Ltd	Mr CJ Meintjies	PO Box 13009 Cascades 3202	033 347 1841	033 347 1845
Verni Speciality Construction Products	Mr VP Botha	PO Box 75393 Garden View 2047	086 118 3764	086 128 3764
Group 5 KZN	Mr G Chambers	PO Box 201219 Durban North 4019	031 569 0300	031 569 0420
SSL Structural Systems Africa (Pty) Ltd	Dr P Heymans	PO Box 1750 Bedfordview	011 409 6700	011 409 6789
Allied Concrete Products	Ms A Allie	PO Box 888 Maitland 7404	021 511 2161	021 511 6571
Hartbeespoort Ready Mix	Mr G Mitchell	PO Box 1232 Brits 0250	012 258 0650/1	012 258 0652
Structural Solutions cc	Mr R Govoni	PO Box 40295 Walmer 6065	041 581 3210	041 581 3126
UWP Consulting	Dr A-C Brink	PO Box 13888 Cascades 3202	033 347 7900	033 347 7950
Bapedi Civil & Structural Consultants	Mr B Kunutu	PO Box 412689 Craighall 2024	011 326 3227	011 326 3363

DATE	CONCRETE SOCIETY OF SOUTHERN AFRICA — INLAND BRANCH EVENTS 2010		
	MEETING/EVENT	VENUE	CONVENOR
04 Feb	Branch Committee meeting	C&CI, Waterfall Park, Midrand	John
04 Mar	Branch Committee meeting/AGM/Carbon Footprint presentation	TBA	John/Hanlie
01 Apr	Branch Committee meeting	C&CI, Waterfall Park, Midrand	John
06 May	Branch Committee meeting	C&CI, Waterfall Park, Midrand	John
14 May	Egg Protection Device Competition – test date and prize-giving	PPC Jupiter Carousel, JHB	Johan van Wyk
20 May	Mini-seminar – Architectural Concrete	TBA	Hanlie
03 Jun	Branch Committee meeting	C&CI, Waterfall Park, Midrand	John
01 Jul	Branch Committee meeting	C&CI, Waterfall Park, Midrand	John
03/04 Aug	National Concrete Seminar	Gauteng	All
12 Aug	Branch Committee meeting	C&CI, Waterfall Park, Midrand	John
02 Sep	Branch Committee meeting	C&CI Waterfall Park, Midrand	John
18 Sep	Annual Concrete Boat Race Day	Victoria Lake, Germiston	Trevor
07 Oct	Branch Committee meeting	C&CI, Waterfall Park, Midrand	John
21 Oct	Mini-seminar- Innovation in South African concrete	TBA	Hanlie
04 Nov	Branch Committee meeting	C&CI, Waterfall Park, Midrand	John
05 Nov	Chairman's Breakfast & Concrete Achiever of the year Award	To be advised	Johan

DATE	INTERNATIONAL EVENTS CALENDAR 2010		
	MEETING/EVENT	VENUE	CONVENOR
14 – 16 April	Design and Construction of Safe and Sustainable High-rise Structures	Technical University, Munich, Germany	Prof Dr HR Viswanath
22 - 24 September	34th IABSE Symposium "Large Structures and infrastructures for Environmentally Constrained and Urbanised Areas"	Venice, Italy	IABSE Organising Committee

DATE	CONCRETE SOCIETY OF SOUTHERN AFRICA NATIONAL OFFICE 2010		
	MEETING/EVENT	VENUE	CONVENOR
28 February	Closure of Source Book Entries Submissions	Distributed to all members	Natasja Pols Administrator of CSSA
11/12 March	National AGM	Cape Town (venue to be confirmed)	Francois Bain President of CSSA
Mid April	Concrete Beton - Issue 124	Distributed to all members	Crown Publications
May	Concrete Flooring Roadshow Seminar	Johannesburg, Durban, Port Elizabeth & Cape Town (venues to be confirmed)	Seminar Organising Committee
Mid May	Distribution of 2010/2011 Source Book	Distributed to all members	Crown Publications
3/4 August	Sustainability Symposium	Johannesburg (venue to be confirmed)	Symposium Organising Committee